Separatrix crossing and large scale diffusion in low-frequency three-wave systems

B. Weyssow,[1] J. D. Reuss,[2] and J. Misguich[2]
[1]*Association Euratom–Etat Belge, Physique Statistique et Plasmas, Université Libre de Bruxelles, Campus Plaine, Code Postal 231, B-1050 Bruxelles, Belgium*
[2]*Association Euratom–CEA sur la Fusion, DRFC, CEA Cadarache, F-13108, Saint-Paul-lez-Durance Cedex, France*
(Received 15 April 1998)

The $\mathbf{E}\times\mathbf{B}$ guiding center diffusion in three low-frequency two-dimensional electrostatic waves is considered. It is shown that the stochastic guiding center (GC) diffusion can be explained and predicted with the help of the rules of the adiabatic theory of Hamiltonian systems, i.e., (i) conservation of the canonical action except at separatrix crossing times and (ii) time evolution of the canonical action determined by the surfaces enclosed by the separatrices of the potential. The probability distributions are calculated. Our demonstration applies at least for isotropically distributed wave vectors, very high Kubo number K, and closed equipotentials. A statistical analysis of the dynamics shows that the GC motion is a *spaced constrained random walk* governed by a ''complete trapping'' scaling law for diffusion: $\overline{D}(K)=K^0$. This result is demonstrated both semianalytically and numerically. [S1063-651X(98)06509-X]

PACS number(s): 52.20.−j, 52.35.−g, 52.65.−y

I. INTRODUCTION

Electromagnetic fluctuations are known to be important for charged particle diffusion in magnetically confined plasmas. The stochastic $\mathbf{E}\times\mathbf{B}$ guiding center (GC) motion in a two-dimensional (2D) low-frequency electrostatic turbulence perpendicular to the strong magnetic field $\mathbf{B}$ has been reconsidered recently by Isichenko *et al.* [1] (see also [2]). An unexpected ''percolation'' scaling law has been provided by $\overline{D}(K)=K^{\gamma}$ with $\gamma=0.7$ for the adimensional diffusion coefficient as a function of the Kubo number K. Here K is the ratio of an average electric drift velocity $v_d=c|E|/B$ to an average phase velocity. This prediction, quite different from that of the Gaussian statistical theories ($\gamma=1$) [3], has been verified numerically in a range of large Kubo numbers (low frequencies) by different authors: a result $\gamma\approx 0.8$ is given in [4] with 64 waves of random amplitudes, whereas $\gamma\approx 0.7$ is reported with a very large number of waves in [5] (with a pure k^{-3} spectrum) and in [6] (with a Gaussian spectrum at small wave vectors and a k^{-3} spectrum at large wave vectors). In the latter simulations, the electrostatic potential is represented as a sum of randomly phased waves [7,8]:

$$H\sim\Phi(x,y,t)\sim\sum_n p(k_n)\sin(\mathbf{k}_n\cdot x-\omega_n t+\phi_{\mathbf{k}_n}) \qquad (1)$$

with $p(k_n)$ given by the k spectrum of drift-wave turbulence. Usually a unique frequency $\omega_n=\omega_0$ is considered for all the waves. Thus, with a large number of waves, numerical simulations at high Kubo numbers generally verify the percolation scaling $\gamma=0.7$, as well as a recent statistical theory based on conditional probabilities [9].

In a small number of waves, however, the exponent $\gamma=0.7$ has generally *not* been observed (the result $\gamma\approx 0.8$ [4] has been obtained with 64 waves of random amplitudes). For example, a result $\gamma=0.92$ has been obtained in [10] for the six-wave Hamiltonian:

$$H(x,y,t)=-\frac{c}{B}\Phi_0\sum_{i=1}^{6}\sin(\omega_i t+\phi_i)\sin(\mathbf{k}_i\cdot\mathbf{x}+\theta_i), \qquad (2)$$

where the phases ϕ_i and θ_i as well as the directions α_i of the wave vectors $\mathbf{k}_i=(k_i\cos\alpha_i, k_i\sin\alpha_i)$ were taken at random in [0,1]. The frequencies were chosen noncommensurable and of the same order: $\omega_i=(1+i/5)^{1/2}\omega_0$, and Φ_0 is an amplitude factor determining the control parameter K. Wave numbers k_i proportional to the frequencies ω_i are considered to model a linear wave dispersion. A scaling $\overline{D}\approx\epsilon$ linear in the control parameter ϵ has been obtained in Ref. [11] for the Hamiltonian

$$H(x,y,t)\sim \sin x\,\cos y+\epsilon\,\sin(kx+\theta_x)\cos(qy-\omega_0 t+\theta_y). \qquad (3)$$

Other values of the scaling exponent were also reported. A result $\overline{D}_{xx}=2\epsilon$ was calculated in Ref. [12] for a Hamiltonian of the form

$$H(x,y,t)\sim \sin x\,\sin y+\epsilon y\,\cos t, \qquad (4)$$

which in coordinates (x,y) is nonperiodic in the y direction. But, in canonical coordinates $x'=x-\sin t$, $y'=y$, the Hamiltonian becomes periodic in both directions:

$$H(x',y',t)\sim \sin(x'-\epsilon\,\sin t)\sin y'. \qquad (5)$$

The phase space has fixed separatrices, i.e., noncrossable lines at $y'=\pm\pi/2$, but also moving (thus crossable) separatrices in the perpendicular direction, making the motion highly nonisotropic. Furthermore, for small values of ϵ and because of the periodicity in t, the structure of the Hamiltonian is only slightly perturbed. [These Hamiltonians (3) and (4) are quite different from the wave Hamiltonians (1) and (2), the sign of which reverses periodically.] A four-wave Hamiltonian [13]

$$H(x,y,t) \sim \tilde{\phi}[\sin x \cos y + \epsilon \cos(kx)\cos(qy-\omega t)] \quad (6)$$

yields the scaling $\overline{D}(\tilde{\phi}) \approx \tilde{\phi}^{0.8}$ at large $\tilde{\phi}$ with the parameters $k=\epsilon=1$ and $q=\omega=2$.

The study developed below of the GC motion in low-frequency waves applies quite generally to the randomly phased wave potential, each having its own phase velocity. The main restriction is that the potential should be free of infinitely long equipotentials.

We prove below that the $\mathbf{E}\times\mathbf{B}$ GC dynamics in electrostatic waves with very low frequencies is governed by the separatrix crossings, i.e., by the time evolution of the surfaces areas enclosed by the separatrices of the potential (named ''domains'' in the phase space) provided they change faster than the canonical action of the well-trapped GC. We also show that in the case of a potential having a series of regularly spaced moving separatrices the diffusion coefficient follows the ''complete trapping'' scaling $\overline{D}(K) = K^0$, i.e., the scaling obtained in [12] for the Hamiltonian (4). In this case it is the canonical action of the well-trapped GC that changes faster than the surfaces areas of the phase space domains (actually, in this case, the surfaces areas of the domains do not change at all). A complete trapping scaling has also been obtained analytically in a 1D problem by using conditional probabilities [14] (see also [15]).

We consider here the large scale $\mathbf{E}\times\mathbf{B}$ motion in three low-frequency electrostatic waves as a simplified representation of a randomly phased wave potential. This type of model has already been considered in [16–18]. It has been shown in [17] and [18] that such simple models are useful to study the Hamiltonian dynamics in case of multiple separatrix crossings and for checking the numerical integration of the equations of motion (which can be performed with a symplectic integrator [20] or with a non-Hamiltonian scheme [21]). Contrary to our previous three waves model [17] , here all the separatrices are moving in the phase space. Thus, the GC are now allowed to visit the whole phase space instead of being enclosed in a single squared domain of the phase space. Here, we analyze the possibility of large scale diffusion in a slowly varying three wave Hamiltonian. The GC motion is described as a sum of a two types of displacements, a first one from phase space domains to neighboring ones and a second one describing the changes of the GC positions inside the domains. The latter motion has already been explained in [17] and [18] where, using a statistical method, the problems related to the very large number of separatrix crossings have been overcome. In the present work the former motion is described statistically and derived from the time evolution of a probability distribution. The main feature of our method is the transformation of the continuous dynamics into a discrete dynamics on gridpoints where the motion reduces to a *spaced constrained random walk* similar to the one discussed by [19], i.e., a random walk where only few directions and lengths for the displacements are allowed. In our case, the constraints are closely related to the rules determining the separatrix crossings.

In Sec. II, we define the three wave Hamiltonian and discuss the structure of the potential: position of the separatrices and areas of the domains in phase space. In the next section, we discuss a few simple rules permitting us to follow the GC motion with a quite good accuracy. These rules are used to show that the stroboscopic trajectories in a periodic box in the phase space for high Kubo number are very close to the trajectories of the frozen Hamiltonian (trajectories in the Hamiltonian at a fixed time). In Sec. IV, we define what we call an equivalent phase space and define the rules for large scale motion induced by separatrix crossings. In Sec. V, we give our conclusions.

II. GUIDING CENTER MOTION IN A THREE WAVE HAMILTONIAN SYSTEM

The analytic description of the charged particle motion in strong magnetic field can be simplified by applying an averaging transformation to remove the high frequency gyration of the particle around the magnetic field lines. Considering a straight and homogeneous magnetic field, i.e., $\mathbf{B}=B\mathbf{1}_z$ and the absence of an electric field in the $\mathbf{1}_z$ direction, the averaged motion, called the GC motion, reduces to a free flight along the magnetic field and to a slow motion in a direction perpendicular to both the electric $\mathbf{E}(x,y,t)$ and the magnetic fields. The resulting equations of motion are known as the $\mathbf{E}\times\mathbf{B}$ GC motion, which reads

$$\frac{d}{dt}\mathbf{Y} = U\mathbf{b} + \frac{c}{B}\mathbf{E}(x,y,t)\times\mathbf{B}, \quad (7)$$

where $\mathbf{Y}=x\mathbf{1}_x+y\mathbf{1}_y+z\mathbf{1}_z$ is the GC position and U is a *constant* velocity parallel to the main magnetic field $\mathbf{b}=\mathbf{B}/B$. In the plane perpendicular to $\mathbf{B}$ the dynamics is obviously a Hamiltonian with

$$H(x,y,t) = -(c/B)\Phi(x,y,t) \quad (8)$$

and

$$\mathbf{E}(x,y,t) = -\nabla\Phi(x,y,t). \quad (9)$$

Here, x and y are canonically conjugated coordinates. This Hamiltonian system is a first-order approximation to the GC motion in an electrostatic turbulence, e.g., a drift wave turbulence of fusion plasmas.

From the point of view of Hamiltonian systems, the low frequency limit is very peculiar. It is well known that in this case an adiabatic invariant exists and the $1\frac{1}{2}$ Hamiltonian system is nearly integrable. This fact has not been included in previous theories. We shall prove below that the $\mathbf{E}\times\mathbf{B}$ GC dynamics in very low frequency electrostatic waves is governed by the mechanism of separatrix crossings.

We consider the following three-wave electrostatic potential $\Phi(\overline{x},\overline{y},\overline{t})$:

$$\Phi(\overline{x},\overline{y},\overline{t}) = 2\pi\Phi_0\{\sin[\overline{y}+\overline{t}] + \sin[\cos(\pi/6)\overline{x} - \sin(\pi/6)\overline{y} + \tfrac{3}{2}\overline{t}] + \sin[-\cos(\pi/6)\overline{x} - \sin(\pi/6)\overline{y} + \tfrac{1}{2}\overline{t}]\}, \quad (10)$$

where Φ_0 is an amplitude and $\{\overline{x},\overline{y},\overline{t}\}$ are dimensionless spatial and time coordinates reduced by k_0 and ω_0, and the equations of motion are

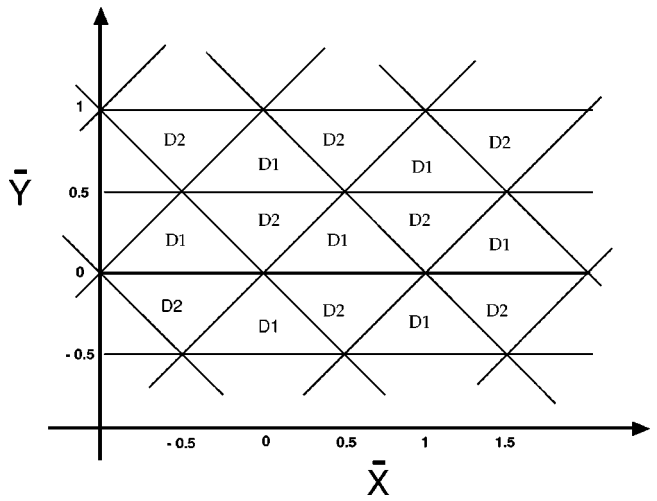

FIG. 1. Separatrices of the Hamiltonian (8) represented at time $\bar{t}=0$ showing two different domains $D1$ and $D2$.

$$\frac{d\bar{x}}{d\bar{t}}=-K\frac{d\bar{\Phi}}{dy},\quad \frac{d\bar{y}}{d\bar{t}}=K\frac{d\bar{\Phi}}{dx}, \tag{11}$$

where $\bar{\Phi}=\Phi/\Phi_0$. The parameter $K=c\Phi_0 k_0^2/B\omega_0$ is the Kubo number. The dimensionless Hamiltonian is simply $\bar{H}(\bar{x},\bar{y},\bar{t})=\bar{\Phi}(\bar{x},\bar{y},\bar{t})$. The wave vectors and wave frequencies are chosen to satisfy five main conditions on the geometrical structure of the potential, namely, (i) we impose that for all times all equipotentials are closed curves, (ii) the potential has no fixed (time independent) straight separatrices, (iii) the potential is spatially periodic (this condition is needed for developing the semianalytical analysis of the GC diffusion), (iv) the wave vectors are chosen isotropic in the (x,y) plane, and (v) the potential is periodic in time.

These constraints are sufficient to avoid the possibility of trapping the guiding centers. The lowest value of the Kubo number considered in our numerical investigations is $K=500$, an already high value compared with that of [7] and [5].

The structure of the potential (10) at various times $\bar{t}/2\pi=0$, $\bar{t}/2\pi=1/30$, $\bar{t}/2\pi=1/12$ is shown in Fig. 1, 2, and 6, respectively. The notations used in the figures are $\bar{T}=\bar{t}/2\pi$, $\bar{X}=\bar{x}/[2\pi\cos(\pi/6)]$, and $\bar{Y}=\bar{y}/2\pi$. The phase space is divided in periodic cells by three sets of straight separatrices defined by

$$\bar{y}=2\pi n_1+2\bar{t},\quad -\sin\left(\frac{\pi}{3}\right)\bar{x}+\frac{1}{2}\bar{y}=2\pi n_2-\frac{3}{2}\bar{t},$$
$$\sin\left(\frac{\pi}{3}\right)\bar{x}+\frac{1}{2}\bar{y}=2\pi n_3-\frac{5}{2}\bar{t}, \tag{12}$$

where n_1,n_2,n_3 are integers.

At time $\bar{t}=0$ (Fig. 1) the three separatrices of the potential cross at a single point, dividing the phase space in triangles all similar in shape and all having the same surface area. These triangles or *domains* in the phase space are denoted $D1$ or $D2$ according to the sign of the potential. At a later time, e.g., $\bar{t}/2\pi=1/30$ (Fig. 2), the triangles of the set

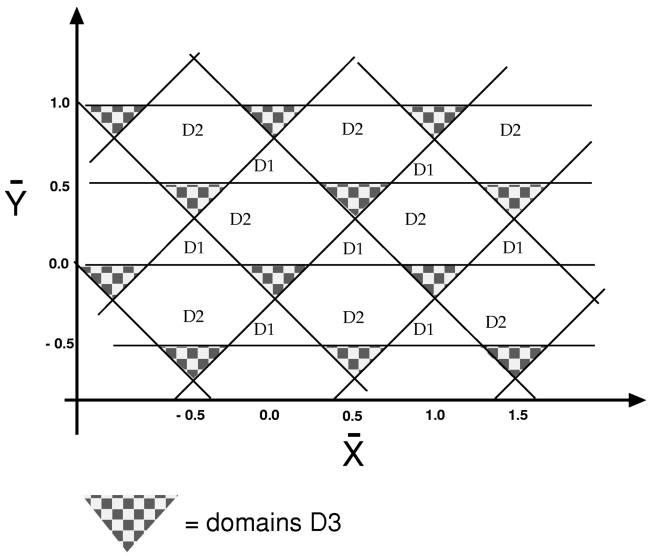

FIG. 2. Separatrices of the Hamiltonian (8) represented at time $\bar{t}/2\pi=1/30$ showing the domains $D1$ and $D2$ and the new domains $D3$. A comparison with Fig. 1 shows a displacement of the domains along the $-x$ and $+y$ directions.

$D1$ have a smaller surface area than at time $\bar{t}=0$ whereas the domains of the set $D2$ now have a hexagonal shape and have larger surface area. The crossing points of the three separatrices at $\bar{t}=0$ are the initial points of a new set of domains $D3$. At $\bar{t}/2\pi=1/12$ (see Fig. 6) the structure of the potential is given by a regular hexagon (domains $D2$) encircled by an ensemble of identical triangles of the sets $D1$ and $D3$. From time $\bar{t}=2\pi/12$ to $\bar{t}=2\pi/6$ the process continues until the triangles $D1$ disappear and are replaced by new domains $D4$. Analyzing the equations of the separatrices, we see that the structure of the potential is recovered each $\bar{t}=2\pi/6$ but with shifted positions. For instance, the intersection point of the separatrices $\{\bar{x},\bar{y}\}=\{-2\pi/12,2\pi/3\}$ at time $\bar{t}=2\pi/6$ is the closest to the intersection point $\{\bar{x},\bar{y}\}=\{0,0\}$ at time $\bar{t}=0$. The domains are thus moving horizontally and vertically at a speed $\bar{v}_x\equiv\bar{x}/\bar{t}=(-1/2)/\cos(\pi/6)$ and $\bar{v}_y\equiv\bar{y}/\bar{t}=2$, respectively. The surface area of the domains can also be evaluated with the help of Eqs. (12). In the time interval $\bar{t}=0$ to $\bar{t}=2\pi/6$ the surface area S_1, S_2, and S_3 of the domains $D1$, $D2$, and $D3$ are given, respectively, by

$$S_1=\frac{(2\pi)^2}{2\cos(\pi/6)}\left(1-6\frac{\bar{t}}{2\pi}\right)^2,$$
$$S_2=\frac{(2\pi)^2}{2\cos(\pi/6)}\left[2-\left(1-6\frac{\bar{t}}{2\pi}\right)^2-\left(6\frac{\bar{t}}{2\pi}\right)^2\right], \tag{13}$$
$$S_3=\frac{(2\pi)^2}{2\cos(\pi/6)}\left(6\frac{\bar{t}}{2\pi}\right)^2.$$

To get the surface area in the next time interval $\bar{t}=2\pi/6$ to $\bar{t}=4\pi/6$, the indexes in Eqs. (13) must be shifted by one unit and the time increased by $2\pi/6$. The surface area of the

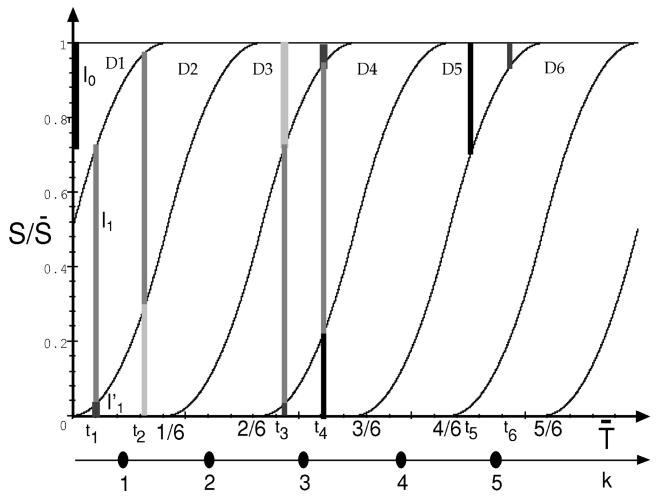

FIG. 3. Time evolution of the surface areas of the domains of the phase space represented during 1/2 of the period. The dynamics of a GC with initial condition in domain $D1$ and canonical action $I_0=0.28$ is also shown. Times $t_1, t_2, \ldots, t_n$ are separatrix crossings times, i.e., times at which the area of the domain containing the GC is equal to the canonical action of the GC.

domains $D2$, $D3$, and $D4$ in the time interval $\bar{t}=2\pi/6$ to $\bar{t}=4\pi/6$ are thus given, respectively, by

$$S_2=\frac{(2\pi)^2}{2\cos(\pi/6)}\left[1-6\left(\frac{\bar{t}}{2\pi}-\frac{1}{6}\right)\right]^2,$$

$$S_3=\frac{(2\pi)^2}{2\cos(\pi/6)}\left\{2-\left[1-6\left(\frac{\bar{t}}{2\pi}-\frac{1}{6}\right)\right]^2-\left[6\left(\frac{\bar{t}}{2\pi}-\frac{1}{6}\right)\right]^2\right\}, \tag{14}$$

$$S_4=\frac{(2\pi)^2}{2\cos(\pi/6)}\left[6\left(\frac{\bar{t}}{2\pi}-\frac{1}{6}\right)\right]^2.$$

This process continues forever, new domains denoted with larger index $D5$, $D6, \ldots$ with surface area S_5, $S_6, \ldots$ replacing the disappearing ones. We note that a periodicity cell of the potential has surface area $\bar{S}=(2\pi)^2/[\cos(\pi/6)\sin(\pi/6)]$. The time evolution of the surface area of the domains in phase space is summarized in a single graph (Fig. 3), where the vertical axis represents the surface of the domains whereas the horizontal axis is the time axis.

The surface area of a domain is measured vertically either between two ''s'' curves or between an ''s'' curve and one of the horizontal lines. At the starting time $\bar{t}=0$, only two types of domains (domains $D1$ and $D2$) fill the phase space.

Considering the very low frequency limit of the wave evolution and, because of the Hamiltonian nature of the equations of motion, the GC displacement follows a small number of very simple rules (first proposed in [22], see also [23]).

(i) A separatrix crossing is an instantaneous event. This is a good approximation for very large Kubo number K (or equivalently very small wave frequencies) since the motion along a separatrix is performed in a very short time interval compared to the time interval between two separatrix crossings.

(ii) The canonical action is conserved except at separatrix crossing times, meaning that the surfaces enclosed by the trajectories are constant whereas the surfaces enclosed by the separatrices are not.

(iii) The separatrix crossing occurs when the surface enclosed by the separatrix of the domain containing the GC is equal to the surface enclosed by the trajectory of the GC.

(iv) The new domain has constant or increasing area.

For example, a GC starting at $\bar{t}=0$ from domain $D1$ with the canonical action equal to the area of this domain will immediately quit his domain. All the *six* domains surrounding each domain $D1$ have increasing area and are thus able to capture the GC. Each of the three smallest domains could capture the GC with probability $p_{1\to3}\equiv(1/3)(dS_3/d\bar{t})/(dS_1/d\bar{t})$, whereas the three largest domains could capture the GC with probability $p_{1\to2}\equiv(1/3)(dS_2/d\bar{t})/(dS_1/d\bar{t})$. Recalling Eqs. (14), the transition probabilities for $\bar{t}/2\pi$ in the interval $[0,1/6]$ are readily evaluated:

$$p_{1\to3}=p\equiv\left|\frac{dS_2}{d\bar{t}}\Big/\frac{dS_1}{d\bar{t}}\right|=\frac{(1-12\bar{t}/2\pi)}{(1-6\bar{t}/2\pi)}, \tag{15}$$

$$p_{1\to2}=q\equiv\left|\frac{dS_3}{d\bar{t}}\Big/\frac{dS_1}{d\bar{t}}\right|=\frac{6\bar{t}/2\pi}{(1-6\bar{t}/2\pi)}. \tag{16}$$

At $\bar{t}=0$, $p_{1\to2}=0$ and the GC is necessarily captured (with probability 1/3) by one of the (three) domains $D2$ (provided the GC is captured by the nearest neighbor). It is also worth noting that rules (i)–(iv) do not depend on the Kubo number. This implies that the GC dynamics, governed by the separatrix crossings, is considered to be in a *saturated regime* for large Kubo numbers: the dynamics is insensitive to changes in the value of the Kubo number (or in the wave frequency). We therefore expect that the GC diffusion will follow a complete trapping scaling law, i.e., $\bar{D}(K)=K^0$.

Let us consider a GC initially in one of the domains $D1$ with a canonical action I_0 smaller than the area of its domain. The behavior of this GC is depicted in Fig. 3. At time t_1 the canonical action of the GC is equal, for the first time, to the surface of domain $D1$. According to rule (iii) the GC performs a separatrix crossing to reach either one of the domains of the set $D2$ or one of the set $D3$, respectively, with a probability p or q divided by the number of accessible domains (i.e., three in the case of transitions to first neighbors and for each set, see Figs. 1, 2, and 6), and canonical action I_1 or I'_1 (with $I'_1<I_1$). This event is a first kind (denoted $T1$) of separatrix crossing. At time $t_2=2\pi/6-t_1$ (see Fig. 2) the canonical action of the GC could be equal to the surface area of the domains $D2$. If this happens, the GC performs a new separatrix crossing (of type $T2$), which brings it *with probability 1* into one of the three nearest domains $D3$ and with new canonical action I_0 (its initial one). At time $t_3=4\pi/6+t_1$ (see Fig. 3) the canonical action I_0 equals the surface area of domain $D3$. The GC having this action performs a separatrix crossing (of type $T1$) to one of the three nearest domains $D4$ or to one of the three nearest domains $D5$ with a probability given, respectively, by $p/3$ or $q/3$ and new canonical actions I_1 or I'_1. Thus, with the help

TABLE I. Separatrix crossing times, canonical actions, and transition probabilities of the first five separatrix crossings. The separatrix crossings t_5 to t_8 are similar to the separatrix crossings at t_1 to t_4. A set of four separatrix crossings thus defines a fundamental periodicity in the diffusion mechanism.

Crossing time	Domain name	Canonical action	Transition probability
0	$D1$	I_0	
$t_1<2\pi/12$	$D1\rightarrow D2$	$I_0\rightarrow I_1$	$p/3$
	$D1\rightarrow D3$	$I_0\rightarrow I_1'$	$q/3$
$t_2=2\pi/6-t_1$	$D2\rightarrow D3$	$I_1\rightarrow I_0$	1/3
$t_3=4\pi/6+t_1$	$D3\rightarrow D4$	$I_0\rightarrow I_1$	$p/3$
	$D3\rightarrow D5$	$I_0\rightarrow I_1'$	$q/3$
$t_4=6\pi/6-t_1$	$D3\rightarrow D5$	$I_1'\rightarrow I_0$	1/3
	$D4\rightarrow D5$	$I_1\rightarrow I_0$	1/3
$t_5=8\pi/6+t_1$	$D5\rightarrow D6$	$I_0\rightarrow I_1$	$p/3$
	$D5\rightarrow D7$	$I_0\rightarrow I_1'$	$q/3$

of Fig. 3, we are able to identify the times of occurrence of the separatrix crossings and the sets of domains where the GC is moving to. This evolution for the first five separatrix crossings is shown in Table I. The table gives the times of separatrix crossings, the name of the domains after a separatrix crossing, the new values of the canonical action, and the transition probability to perform a jump to a new domain. The GC dynamics depicted here is valid for a specific initial condition, defined by the initial domain $D1$ and the initial canonical action I_0, because as we see here, most of the separatrix crossings are performed with transition probabilities q and p determined by the initial state of the GC.

We observe that the canonical action of the GC at stroboscopic times $\bar{t}=4\pi n$ (n is an integer) switches between the initial canonical action and a second value, the *complementary* canonical action I_1'. As a consequence, at stroboscopic times, the positions of the GC are the points of *two* trajectories of the frozen Hamiltonian (i.e., the trajectories of the Hamiltonian with $\bar{t}$ considered as a constant) that enclose a surface whose area equals either the initial canonical action of the GC or the *complementary* canonical action I_1'. The randomness of the GC trajectory is in fact strongly spatially constrained because, as we see here, the GC must be on specific trajectories of the frozen Hamiltonian at periodic times.

The relationship between one stroboscopic trajectory with two trajectories of the frozen Hamiltonian (at time $\bar{t}=0$) is shown in Fig. 4, where we show the numerical solution of the equations of motion at large Kubo number (here $K=500$) and in Fig. 5, where the same points, brought back in a single moving periodicity box of the phase space, determine two distinct trajectories of the frozen in time Hamiltonian. To observe numerically this property of the three waves Hamiltonian, the equations of motion of motion (11) were solved using a fourth-order Runge-Kutta (RK) method. As in [18], the statistics of events (the values of the transition probabilities) is not exactly the expected one but the accuracy of the integrator seems sufficient for our purpose. At Kubo number $K=10^3$, a stroboscopic point is obtained after 4×10^6 iterations of the RK. Most of the results were obtained with an Alpha computer and a CRAY J916 computer. The numerical simulations performed over 1000 periods of the potential for 64 initial conditions were obtained on a CRAY T3E computer and required about 8h CPU time on each of the 64 processors. The accuracy of the numerical results can be checked from the stroboscopic plots of the GC trajectories. The case of the GC starting in domain $D1$ with a canonical action slightly smaller than the surface of its homing domain is typical of the behavior of all the trajectories.

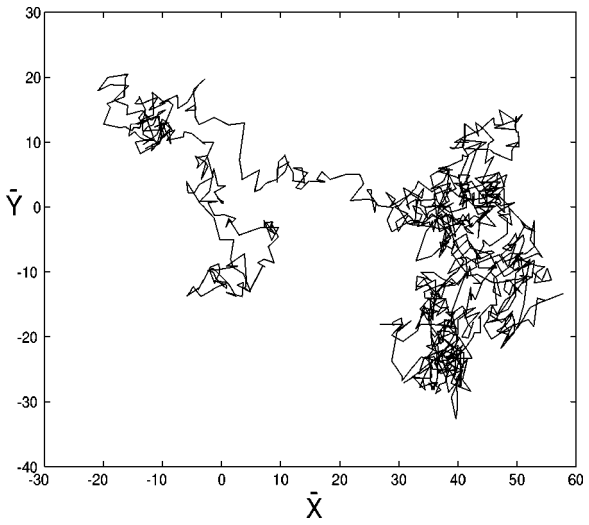

FIG. 4. A GC stroboscopic trajectory (1000 periods, Kubo number $K=1000$). The initial condition is $\bar{X}=0.375/2\pi$, $\bar{Y}=0.75/2\pi\ \cos(\pi/6)$.

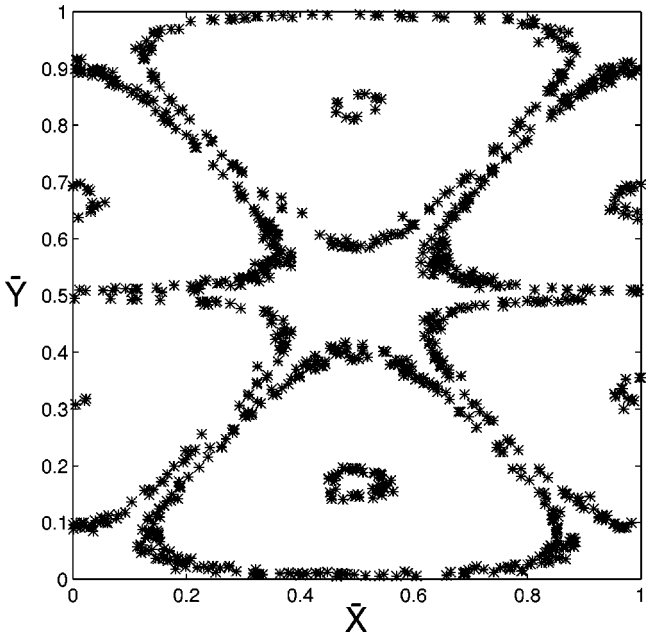

FIG. 5. The positions of the GC of Fig. 4 at stroboscopic times (1000 periods) shown in a reference moving square reproduce the trajectories of the frozen Hamiltonian. One initial condition gives a trajectory corresponding to the initial GC canonical action plus a second trajectory corresponding to a complementary canonical action (small circles).

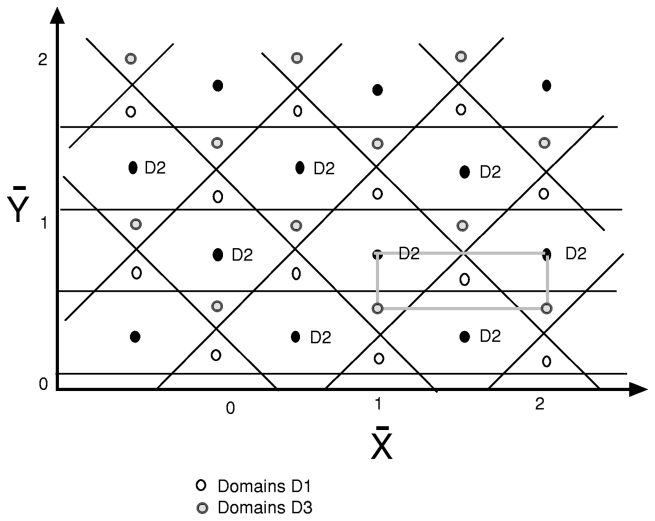

FIG. 6. Representation of the domains of the phase space at time $\bar{t}/2\pi = 1/12$, i.e., $k=1$ and their elliptic point.

III. A SEMIANALYTICAL ESTIMATE OF THE DIFFUSION COEFFICIENT

We now briefly report a method for (i) determining probabilistically the domains that could be visited by the GC at a certain time and (ii) evaluating the diffusion coefficient from the GC dynamics, i.e., from the separatrix crossings.

In this method, each domain of the phase space with its full structure (Fig. 6) is replaced by its elliptic point (Fig. 7). These points are distributed regularly in the phase space due to the periodicity of the potential. The best realization is obtained at times $\bar{t}/2\pi = (-1+2k)/12$ (where k, the *equivalent phase space time*, is a positive integer) when all the triangles in the phase space have the same shape and size (Fig. 6). In this representation, a GC displacement reduces to a jump from one gridpoint to another. The integer k can be used to count the number of separatrix crossings or can be used as a measure of time as can be seen in Fig. 3. The directions of the jumps are determined by the rules for a separatrix crossing, i.e., they are performed in directions given by the positions of the elliptic points of the domains having increasing surface area (the separatrix crossings are spaced constrained jumps). The coordinates of a point in the grid m,n are chosen in such a way that at $k=1$ the points $\{m,n\}=\{2a+3,4b+3\}$, where a and b are arbitrary integers, correspond to the domains $D1$ whereas the points $\{m,n\}=\{2a+2,4b+2\}$ correspond to the domains $D2$ and the points $\{m,n\}=\{2a+1,4b+3\}$ correspond to the domains $D3$. All the remaining positions on the grid must be removed from the definition of the equivalent phase space. At the next equivalent phase space time, the domains $D1$ have disappeared and are replaced by the domains $D4$ (see Fig. 3). Therefore, at $k=2$ the points $\{m,n\}=\{2a+3,4b+3\}$ correspond to the domains $D4$ whereas the other points keep their relations to the domains $D2$ and $D3$. At $k=3$ the points $\{m,n\}=\{2a+2,4b+2\}$, previously related to the domains $D2$, now belong to the domains $D5$ and so on.

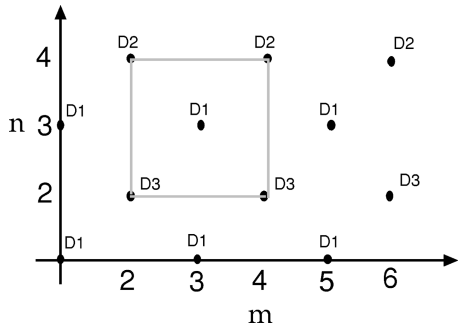

FIG. 7. The equivalent phase space is the set of elliptic points of the domains shown in Fig. 6. The distances are rescaled (essentially by a factor 2 on the vertical axis) for simplicity of the analysis.

The jumps (separatrix crossings) follow the rules $\{n\to n+1, m\to m+1\}$ or $\{n\to n+2, m\to m+2\}$. More specifically, the separatrix crossing of type $T1$ is a jump with probability $p/3$ from a point $\{m,n\}$ to one of the three points $\{m+1,n+1\}$, $\{m-1,n+1\}$, $\{m,n-2\}$ or with probability $q/3$ (recall $p+q=1$) to one of the three points $\{m+1,n-1\}$, $\{m-1,n-1\}$, $\{m,n+2\}$. A separatrix crossing of type $T2$ is a jump with probability 1/3 from a point $\{m,n\}$ to one of the three points $\{m+1,n+1\}$, $\{m-1,n+1\}$, $\{m,n-2\}$.

We now introduce a probability distribution $P(m,n,k)$ of finding a GC at the point m,n at time k. We consider the initial condition $P(m,n,0)=\delta_{m-m_0,n-n_0}$, i.e., the GC is initially at the point $\{m_0,n_0\}$. This initial point could be $\{m,n\}=\{3,3\}$ as in Fig. 7. After the first separatrix crossing, the probability distribution is

$$P(m,n,1)=\frac{p}{3}(\delta_{m-m_0-1,n-n_0-1}+\delta_{m-m_0+1,n-n_0-1}+\delta_{m-m_0,n-n_0-2})+\frac{q}{3}(\delta_{m-m_0-1,n-n_0+1}+\delta_{m-m_0+1,n-n_0+1}+\delta_{m-m_0,n-n_0+2}) \quad (17)$$

since the probability distribution is $p/3$ in three domains $D2$ and $q/3$ in three domains $D2$. With the initial condition $P(3,3,0)=1$, the first separatrix crossing gives $P(4,4,1)=P(2,4,1)=P(3,1,1)=p/3$ and $P(4,2,1)=P(2,2,1)=P(3,5,1)=q/3$. At the second separatrix crossing (of type $T2$) only the part of the probability distribution corresponding to the domains $D2$ changes as shown in Table I. Thus to describe the second separatrix crossing, we need three partial probability distributions, denoted $A(m,n,k)$, $B(m,n,k)$, $C(m,n,k)$, the sum of which reproduces the probability distribution

$$P(m,n,k)=A(m,n,k)+B(m,n,k)+C(m,n,k). \quad (18)$$

The initial conditions are chosen as follows:

$$A(m,n,0)=\delta_{m-m_0,n-n_0}, \quad B(m,n,0)=0, \quad C(m,n,0)=0. \quad (19)$$

Right after the first separatrix crossing, we have

$$P(m,n,1)\equiv(T_p+T_q)A(m,n,0), \quad (20)$$

where

$$T_pA(m,n,0)\equiv\frac{p}{3}\{A(m-1,n-1,0)+A(m+1,n-1,0)+A(m,n+2,0)\},$$

$$T_qA(m,n,0)\equiv\frac{q}{3}\{A(m-1,n+1,0)+A(m+1,n+1,0)+A(m,n-2,0)\}. \quad (21)$$

Similarly, we define the phase space translation T_1:

$$T_1A(m,n,1)\equiv\frac{1}{3}\{A(m-1,n-1,1)+A(m+1,n-1,1)+A(m,n+2,1)\}. \quad (22)$$

Obviously, $T_pA(m,n,0)$ is nonzero on the points corresponding to the domains $D2$ where the GC has the canonical action I_1 and $T_qA(m,n,0)$ is nonzero on the points corresponding to the domains $D3$ where the GC has the canonical action I_1'.

In $A(m,n,k)$, we collect the part of the probability distribution, which changes at each separatrix crossing, i.e., at each time interval $\Delta\bar{t}/2\pi=1/6$, whereas in $B(m,n,k)$ and $C(m,n,k)$ we collect the part of the probability distribution, which changes each two separatrix crossings, i.e., at each time interval $\Delta\bar{t}/2\pi=1/3$. The first separatrix crossing gives

$$A(m,n,1)=T_pA(m,n,0),\quad B(m,n,1)=T_qA(m,n,0),\quad C(m,n,1)=C(m,n,0), \quad (23)$$

where $A(m,n,1)$ and $B(m,n,1)$ are, respectively, the probability density for the GC to be in a domain D_2 and in a domain D_3. At the next separatrix crossing time $t_2=2\pi/6-t_1$, i.e., $k=2$, only the part $A(m,n,1)$ of the probability distribution changes because the separatrix crossing (of type $T2$) is a jump from the domains $D2$ to one of three nearest domains $D3$ (see Table I). The second separatrix crossing leads to

$$A(m,n,2)=T_1A(m,n,1),\quad B(m,n,2)=B(m,n,1),\quad C(m,n,2)=C(m,n,1). \quad (24)$$

The partial probabilities $A(m,n,2)$ and $B(m,n,2)$ are nonzero on the points corresponding to the domains $D3$ but with different canonical actions I_0 and I_1'. For later convenience, this transformation can also be written

$$A(m,n,2)=T_1[T_pA(m,n,0)+C(m,n,0)],\quad B(m,n,2)=T_qA(m,n,0),\quad C(m,n,2)=0. \quad (25)$$

The probability distribution at $k=2$ is shown in Fig. 8, where the values of $P(m,n,2)$ are given at their positions $\{m,n\}$. The arrows indicate the directions of the transfer of probability distribution due to the next separatrix crossing. The arrows represents symbolically a transport of the probability distribution in the phase space; it multiplies the value of the probability distribution at a given point by the transition probability (in this case $p/3$ for the gray arrows and $q/3$ for the black ones as shown in Table I) and transports the obtained value to a new position in phase space. The values of the probability distribution that are transported this way are given in Table II for the first five separatrix crossings.

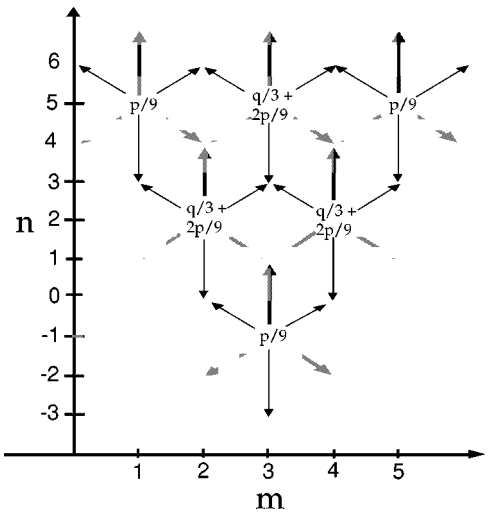

FIG. 8. The probability distribution at the equivalent phase space time $k=0$ and its change due to a third separatrix crossing.

TABLE II. Equivalent phase space times k, domain names, canonical actions, and transfer of probability distribution after the first five separatrix crossings.

k	domain	action	probability distribution
0	$D1$	I_0	1
1	$D2$	I_1	$\frac{p}{3}(1)$
	$D3$	I_1'	$\frac{q}{3}(1)$
2	$D3$	I_0	$\frac{1}{3}\left(\frac{p}{3}\right)$
	$D3$	I_1'	$\frac{q}{3}$
3	$D4$	I_1	$\frac{p}{3}\left(\frac{1}{3}\frac{p}{3}\right)$
	$D5$	I_1'	$\frac{q}{3}\left(\frac{1}{3}\frac{p}{3}\right)$
	$D3$	I_1'	$\frac{q}{3}(1)$
4	$D5$	I_0	$\frac{1}{3}\left(\frac{p}{3}\times\frac{1}{3}\times\frac{p}{3}+\frac{q}{3}\right)$
	$D5$	I_0	$\frac{q}{3}\left(\frac{1}{3}\frac{p}{3}\right)$
5	$D6$	I_1	$\frac{p}{3}\left(\frac{1}{3}\frac{p}{3}\times\frac{1}{3}\times\frac{p}{3}+\frac{q}{3}\right)$
	$D7$	I_1'	$\frac{q}{3}\left(\frac{1}{3}\frac{p}{3}\times\frac{1}{3}\times\frac{p}{3}+\frac{q}{3}\right)$
	$D5$	I_1'	$\frac{q}{3}\left(\frac{1}{3}\frac{p}{3}\right)$

The third ($k=3$) separatrix crossing, of type $T1$, concerns the part of the probability distribution corresponding to domain $D3$, i.e., B does not change. Thus, at time $t_3=4\pi/6+t_1$ we have

$$A(m,n,3)=T_pA(m,n,2),\quad B(m,n,3)=B(m,n,2),\quad C(m,n,3)=T_qA(m,n,2) \tag{26}$$

where $A(m,n,3)$, $B(m,n,3)$, and $C(m,n,3)$ are related, respectively, to the domains $D4$, $D3$, and $D5$ and to GC with canonical actions I_1, I_1', and I_1'.

The fourth separatrix crossing affects all the partial distributions except the one concerning the domains $D5$, i.e., C does not change and we have

$$A(m,n,4)=T_1[A(m,n,3)+B(m,n,3)],\quad B(m,n,4)=0,\quad C(m,n,4)=C(m,n,3). \tag{27}$$

In terms of the initial values, this transformation reads

$$A(m,n,4)=T_1[T_pT_1\{T_pA(m,n,0)+C(m,n,0)\}+T_qA(m,n,0)],\quad B(m,n,4)=0,\quad C(m,n,4)=T_qT_1\{T_pA(m,n,0)+C(m,n,0)\}. \tag{28}$$

and the total probability distribution, after $k=4$ separatrix crossings, is given by

$$P(m,n,4)=A(m,n,4)+C(m,n,4). \tag{29}$$

The next four separatrix crossings are described by the same formulas but with $A(m,n,4)$, $B(m,n,4)$, and $C(m,n,4)$ for new initial values. The whole scenario is summarized in Table II, where the probability distribution $P(m,n,k)$, i.e., the probability to be at the equivalent phase space time k in a given domain with a given canonical action, is given for the first five separatrix crossings and for an initial condition in domain $D1$ and for an initial canonical action I_0.

The transformation (28) is thus a mapping describing the transport across the domains in the phase space. It is now an easy task to show that (i) the probability density defined by the iterative procedure given hereabove leads to a Gaussian distribution and (ii) the mean square displacement is proportional to $\overline{t}$, i.e., the process is diffusive. Here the average of a ''function'' defined on the equivalent phase space is the weighted sum at a given time of the value of the function on all the equivalent phase space points. The mean square displacement is accordingly evaluated as follows:

$$\langle r^2(k)\rangle=\sum_{m,n}(m^2+n^2)P(m,n,k). \tag{30}$$

The iterative procedure is very easily implemented on a computer (a few lines in Matlab language) and permits a very easy evaluation of the mean square displacement. The result is typical of a diffusive process, i.e., a mean square displacement linear in time. The diffusion coefficient derived from Eq. (29) *still depends on the initial value* of the GC canonical action through the transition probabilities p and q. With $p\approx0.66$ and $q\approx0.33$ corresponding to a GC with initial canonical action $I_0=S/16$ the diffusion coefficient of the motion along the m axis (corresponding to the x axis) is $\overline{D}_m\approx6.083$, whereas for $p\approx0.95$ and $q\approx0.05$ the result is $\overline{D}_m\approx7.65$.

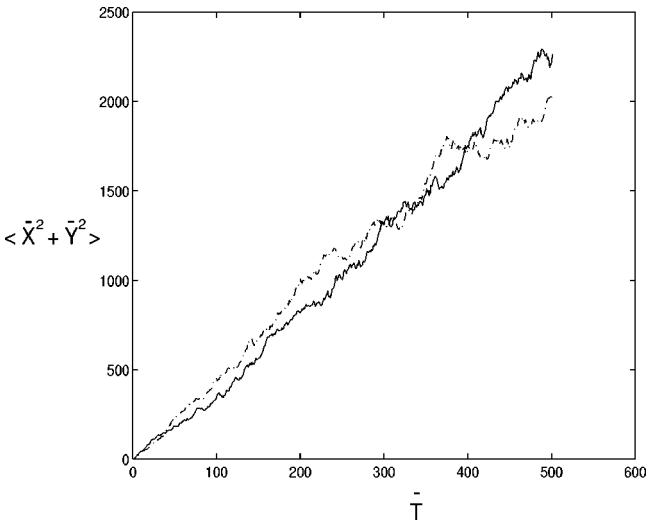

FIG. 9. The mean square displacement $\langle\overline{r^2}\rangle=\langle\overline{x^2}+\overline{y^2}\rangle$ averaged over 64 trajectories with initial conditions taken on a grid in phase space. The initial canonical actions are consequently random numbers. 500 periods are shown. The Kubo numbers are $K=1000$ (continuous line) and $K=500$ (dashed line). The scaling for the dimensionless diffusion coefficients is approximatively $\overline{D}(K)\approx K^0$ and the average numerical value is $\approx2125/500\approx4.25$.

Figure 9 shows a linear increase of the averaged mean square displacement obtained from the numerical solution of the equations of motion performed for 500 periods of the potential and for two different values of the Kubo number: at $K=1000$ (continuous line) and at $K=500$ (dashed line). We observe that the slopes of the mean square displacements (averaged over 64 trajectories), i.e., the dimensionless diffusion coefficients are almost identical: $\overline{D}(K)\approx K^0$.

To facilitate the comparison with the result of the semianalytical method we performed another numerical simulation with 64 GC having different initial positions but the same initial canonical action $I_0=S/16$. In this case, a diffusion coefficient $\overline{D}_x\approx1.90$ along the x axis and a diffusion coefficient $\overline{D}_y(K)\approx1.78$ along the y axis are obtained. The former result is within 15% from the value of the semianalytic calculation: $\overline{D}_x\approx\overline{D}_m\cos^2(\pi/6)/4\approx2.09$. Therefore the semianalytical calculation reasonably represents the numerical results for a given initial action.

IV. CONCLUSIONS

A three wave Hamiltonian has been considered as a simplified model of $\mathbf{E}\times\mathbf{B}$ electrostatic turbulence. We have shown numerically and analytically that for large values of the Kubo number the GC dynamics is controlled by the separatrix crossings, i.e., the canonical action is conserved, the

separatrix crossings are instantaneous, and so on. Using a method that reduces the separatrix crossings to jumps from one gridpoint to another, we have determined iteratively the change in time of the probability density. The mean square displacement and the diffusion coefficient have also been evaluated. We have shown that the GC diffusion in three waves is a random walk with the following properties: (i) the dynamics considered here is not a continuous time random walk (CTRW) because all the separatrix crossings occur at fixed time intervals, (ii) the dynamics is a spaced constrained random walk (see, e.g., [19]) because the separatrix crossings can be reduced to spatial translations of the phase space in directions defined by angles multiples of 30°, and (iii) the probabilities of jumps for two successive separatrix crossings are not independent but the direction of the separatrix crossing is chosen at random. Our semianalytical model of diffusion leads to a complete trapping scaling law, i.e., the dimensionless diffusion coefficient $\overline{D}$ is independent of the Kubo number: $\overline{D}(K)=K^0$. This scaling is valid for very large Kubo numbers.

ACKNOWLEDGMENTS

This work has been done while one of us (B.W.) was at the Center de Recherche CEA, Cadarache (France) with the financial support of a Euratom Mobility grant. Discussions with Dr. F. Spineanu and Dr. M. Vlad and with Professor Y. Elskens are greatly acknowledged.

[1] M. B. Isichenko and W. Horton, Comments Plasma Phys. Control. Fusion **14**, 249 (1991).
[2] A. V. Gruzinov, M. B. Isichenko, and Ya. L. Kalda, Zh. Éksp. Teor. Fiz. **97**, 476 (1990) [Sov. Phys. JETP **70**, 263 (1990)].
[3] T. H. Dupree, Phys. Fluids **10**, 1049 (1967).
[4] M. Ottaviani, Europhys. Lett. **20**, 111 (1992).
[5] J.-D. Reuss and J. H. Misguich, Phys. Rev. E **54**, 1857 (1996).
[6] B. Weyssow and M. De Leener (private communication).
[7] M. Pettini, A. Vulpiani, J.-H. Misguich, R. Balescu, M. De Leener, and J. Orban, Phys. Rev. A **38**, 344 (1988).
[8] M. De Leener, Phys. Rev. E **50**, 502 (1990).
[9] M. Vlad, F. Spineanu, J.-H. Misguich, and R. Balescu, Phys. Rev. Lett. (to be published).
[10] M. B. Isichenko, W. Horton, D. E. Kim, E. G. Heo, and D.-I. Choi, Phys. Fluids B **4**, 3973 (1991).
[11] I. Doxas, W. Horton, and H. L. Berk, Phys. Fluids A **2**, 1906 (1990).
[12] A. A. Chernikov, A. I. Neistadt, A. V. Rogalsky, and V. Z. Yackhnin, Chaos **1**, 206 (1991).
[13] W. Horton, Plasma Phys. Controlled Fusion **27**, 937 (1985).
[14] M. Vlad, J.-D. Reuss, F. Spineanu, and J.-H. Misguich, J. Plasma Phys. (to be published).
[15] J.-H. Misguich, J.-D. Reuss, M. Vlad, and F. Spineanu, EUR-CEA-FC Report No. 1622 (Cadarache, 1998) [Physicalia (to be published)].
[16] J.-H. Misguich and R. Nakach, Phys. Rev. A **44**, 3869 (1991).
[17] B. Weyssow, Phys. Lett. A **22**, 234 (1997).
[18] B. Weyssow, J. Plasma Phys. **59**, 1 (1997).
[19] L. B. Koralov, S. K. Nechaev, and Ya. G. Sinai, Chaos **1**, 131 (1991).
[20] B. Weyssow and M. Eberhard (unpublished).
[21] W. H. Press, B. P. Flannery, S. A. Teukolsky, and W. T. Vetterling, *Numerical Recipes* (Cambridge University Press, Cambridge, 1987).
[22] I. M. Lifshitz, A. A. Slutskin, and V. M. Nabutovskii, Zh. Éksp. Teor. Fiz. **41**, 939 (1961) [Sov. Phys. JETP **14**, 669 (1962)].
[23] A. I. Neistadt, Sov. J. Plasma Phys. **12**, 568 (1986).